Research on Parallel Regenerative Braking Strategy for Hybrid Buses Based on the Adequacy of Energy Recovery

Jinlong Liu[1, a, *], Jiawei Ma[2, b], Wenqi Jiang[3, c]

[1]School of Automotive Engineering, Harbin Institute of Technology, Weihai 264209, China;

[2]School of Engineering, University of Melbourne, Parkville VIC 3010, Australia;

[3]Department of Civil & Environmental Engineering, Imperial College London, London SW7 2AZ, UK

[a]ljl199022@sina.com, [b]samdroid@126.com, [c]wenqi.jiang13@imperial.ac.uk

Abstract. The introduction of Braking Energy Recovery System enables hybrid commercial vehicle to recover partial of its energy during the braking process. In order to increase the recovery rate of the regenerative braking system, parallel brake force distribution strategy of the rear-wheel-drive bus was discussed. The traditional brake force distribution strategy was introduced at first. Then, the shortcomings of the traditional strategy have been improved, thereby enabling the strategy to enhance the recovery rate of regenerative braking and braking performance to a certain extent. MATLAB/SIMULINK platform has been utilized to build and simulate the models of traditional and improved strategies embedded certain parameters. The results show that the revised strategy can recover more energy and decrease the braking distance at the same time.

Keywords: Parallel hybrid commercial vehicles, parallel braking force distribution strategy, regenerative braking, recovery rate, braking distance.

1. Introduction

Under dual pressures from environment and energy crisis, the introduction of regenerative braking system (Regenerative Braking System, RBS) to parallel hybrid electric vehicles (Parallel Hybrid Electric Vehicle, PHEV) is the most effective way to improve the vehicle performance, which is also energy-saving and environmental friendly [1]. Braking energy recovery, which is significant for global energy conservation and environmental protection [2], can greatly improve the energy efficiency of the vehicle and reduce the vehicle's fuel consumption [3]. The operation of Braking Energy Recovery System depends on driving conditions, the structure of systems and control strategies [4]. Besides, the system is also highly related to the characteristics of the battery, the operating characteristic of electromotor, charging speed and other factors [5]. Therefore, considering different conditions, the research of strategy which could fully recover braking energy is not only a breakthrough in technology, but of a great value [6]. Since majority of hybrid commercial vehicles employ rear-wheel-drive pattern, this paper would concentrate on the rear-wheel-drive parallel braking force distribution strategy.

2. Conventional Parallel Braking Force Distribution Strategy

When the rear-wheel-drive of hybrid vehicle is activated, the regenerative braking force is applied to the rear wheels.

$$F_{b\_f\_sum} = F_{b\_f\_me}. \tag{1}$$

$$F_{b\_r\_sum} = F_{b\_r\_me} + F_{b\_r\_re}. \tag{2}$$

As is shown in Eq.1 and Eq.2, $F_{b\_f\_sum}$ is the total breaking force applied on front wheels; $F_{b\_r\_sum}$ is the total breaking force applied on rear wheels; $F_{b\_r\_re}$ is the regenerative braking force of the rear wheels; $F_{b\_f\_me}$ is the mechanical braking force of the front wheels; $F_{b\_r\_me}$ is the mechanical braking force of the rear wheels.

The braking force distribution coefficient of rear-wheel-drive hybrid vehicle can be defined as the ratio of mechanical braking force of the front wheels to the sum of vehicle mechanical braking force and regenerative braking force.

$$\beta_{hev} = \frac{F_{b\_f\_sum}}{F_{b\_f\_sum} + F_{b\_r\_sum}} = \frac{F_{b\_f\_me}}{F_{b\_f\_me} + F_{b\_r\_me} + F_{b\_r\_re}}. \quad (3)$$

As is shown in Eq.3, β_{hev} is the braking force distribution coefficient of rear-wheel-drive hybrid vehicle.

Conventional parallel braking force distribution strategy divides the process of braking into three main parts. When the expected braking severity is less than 0.1, it can be considered as mild braking process; when the expected braking severity is between 0.1 and 0.7 and when the mechanical braking forces have not made the front or rear wheels being in critical locked state， it can be considered as moderate braking process; when the braking severity is higher than 0.7 or the mechanical braking forces have made the front or rear wheels being in critical locked state， it can be considered as severe braking process.

In the process of mild braking, the regenerative braking force is applied on the rear wheels, while front and rear wheels mechanical braking forces are zero.

$$F_{b\_r\_re} = \begin{cases} Mgz_{expect}, & Mgz_{expect} \le F_{re\_a} \\ F_{re\_a}, & Mgz_{expect} > F_{re\_a} \end{cases}. \quad (4)$$

$$F_{b\_f\_me} = F_{b\_r\_me} = 0. \quad (5)$$

As is shown in Eq.4, M is the mass of the vehicle; g is the acceleration of gravity; z_{expect} is the expected braking intensity applied by the driver; F_{re_a} is the maximum braking force provided by the electromotor.

In the process of moderate braking, the mechanical braking force and regenerative braking force are applied simultaneously. The value of the regenerative braking force is restricted by the braking regulations ECE and anti-lock braking of rear wheels. Limitations of braking regulations ECE on the commercial vehicles are reflected in the value of braking force distribution coefficient. The lower limits of breaking force distribution coefficient for rear-wheel-drive hybrid vehicles are shown in Table 1.

Table 1 The minimum of breaking force distribution coefficient

Braking Intensity	Breaking Force Distribution Coefficient
$0.1 \le z < 0.15$	$\left(b + zh_g\right)/L$
$0.15 \le z \le 0.3$	$\max\left\{(z-0.08)\left(b+zh_g\right)/Lz, \left[1-(z-0.08)\left(a-zh_g\right)/Lz\right], \left(b+zh_g\right)/L\right\}$
$0.3 < z \le 0.6$	$\max\left\{\left[1-(z-0.0188)\left(a-zh_g\right)/(0.74Lz)\right], \left(b+zh_g\right)/L\right\}$
$z > 0.6$	$\left[1-(z-0.0188)\left(a-zh_g\right)/(0.74Lz)\right]$

As is shown in Table.1, a is the distance between center of mass and front axle; b is the distance between center of mass and rear axle; h_g is the height of center of mass; L is the wheel base of vehicle; z is the severity of braking.

In order to meet the ECE regulations, the braking force distribution coefficient of rear-wheel-drive hybrid vehicle should meet the regulations in Table 1.

$$F_{b\_r\_re} \le \frac{\left(1-\beta_{hev\_\min}\right)F_{b\_f\_me} - \beta_{hev\_\min}F_{b\_r\_me}}{\beta_{hev\_\min}} = F_{b\_r\_re\_ECE}. \quad (6)$$

As is shown in Eq.6, $\beta_{hev\_\min}$ is the minimum braking force distribution coefficient allowed in ECE regulation.

During the braking process of rear-wheel-drive hybrid vehicle, regenerative braking forces are added to the rear wheels, resulting in the risk of ahead locking of the rear wheels. Therefore, for a

certain value of mechanical braking force of the front wheels, the maximum value of braking force of rear wheels is determined correspondingly.

The constraints of anti-lock rear wheels can be concluded by the R curve.

$$F_{b\_r\_lock} = \frac{\varphi G a}{L + \varphi h_g} - \frac{\varphi h_g}{L + \varphi h_g} F_{b\_f} . \tag{7}$$

$$F_{b\_r\_re} \le F_{b\_r\_lock} - F_{b\_r\_me} = F_{b\_r\_re\_\mathrm{ABS}} . \tag{8}$$

As is shown in Eq.7 and Eq.8, $F_{b\_r\_lock}$ is the maximum braking force on rear wheels allowed by anti-lock rear wheels constraint; $F_{b\_r\_re\_\mathrm{ABS}}$ is the maximum regenerative braking force on rear wheel allowed by anti-lock rear wheels constraint; φ is the pavement friction coefficient; G is the vehicle gravity.

Eq. 9 shows the maximum regenerative braking force which is added on the rear wheels in the moderate braking period.

$$F_{b\_r\_re} \le \min\left\{F_{b\_r\_re\_\mathrm{ECE}}, F_{b\_r\_re\_\mathrm{ABS}}\right\} = F_{b\_r\_re\_\max} . \tag{9}$$

Eq.10 shows the participant regenerative braking force of rear wheels in the moderate braking period.

$$F_{b\_r\_re} = \begin{cases} F_{re\_a}, & F_{re\_a} \le F_{b\_r\_re\_\max} \\ F_{b\_r\_re\_\max}, & F_{re\_a} > F_{b\_r\_re\_\max} \end{cases} . \tag{10}$$

In the severe braking period, only the mechanical braking forces play roles in braking process; the regenerative braking force is zero.

$$F_{b\_r\_re} = 0 . \tag{11}$$

During the whole braking process, the ratio of front mechanical braking force to rear mechanical braking force is a constant value.

$$\beta_{me} = \frac{F_{b\_f\_me}}{F_{b\_f\_me} + F_{b\_r\_me}} . \tag{12}$$

As is shown in the Eq.12, β_{me} is the mechanical braking force distribution coefficient.

It can be concluded from Eq.12 that if the regenerative braking force participate in the braking process, the braking force distribution coefficient of PHEV with rear-wheel drive pattern would be lower than the mechanical braking force distribution coefficient. And if there is no braking force added to the rear wheels during the braking process, the braking force distribution coefficient of PHEV with rear-wheel drive pattern would equal with the mechanical braking force distribution coefficient.

The mechanical braking force distribution is determined by the vehicle parameters and the synchronizing adhesion coefficient.

$$\varphi_0 = \left(L\beta_{me} - b\right) / h_g . \tag{13}$$

As is shown in the Eq.13, φ_0 is the synchronizing adhesion coefficient.

In sum, the mechanical braking force is decided by the driver intention. In the mild braking period, only the regenerative braking forces play roles in braking process. In the moderate braking period, both the regenerative braking forces and the mechanical braking forces play roles in braking process. In the severe braking period, only the mechanical braking forces play roles in braking process.

3. Revised Parallel Strategy

In the traditional parallel strategy, the PHEV can recover lots of energy in the mild braking process; it can recover considerable energy and shorten the braking distance in the moderate braking process; however it can recover little energy in the severe braking process.

If the PHEV is running on the road whose friction coefficient is over 0.7, regenerative braking force on rear wheels can still be added when the PHEV is just at the beginning of the severe braking

period because the mechanical braking forces have not made the front or rear wheels being in critical locked states. If the PHEV is running on the road whose friction coefficient is lower than the synchronizing adhesion coefficient and the mechanical braking forces have made the front wheels being in the critical locked state in the severe braking period, the regenerative braking force can still be added on the rear wheels until the rear wheels slide into the critical locked state.

In order to increase the regenerative braking recovery rate, the novel strategy should be revised in the two mentioned cases.

Eq.14 shows the revised strategy in the mild braking process. In this period, the revised one is the same with the traditional one. The regenerative braking forces are added on rear wheels and the mechanical braking forces of front and rear wheels are zero.

$$\begin{cases} F_{b\_r\_re} = \begin{cases} Mgz_{\exp ect}, & Mgz_{\exp ect} \le F_{re\_a} \\ F_{re\_a}, & Mgz_{\exp ect} > F_{re\_a} \end{cases} \\ F_{b\_f\_me} = F_{b\_r\_me} = 0 \\ F_{b\_f\_sum} = 0 \\ F_{b\_r\_sum} = F_{b\_r\_re} \end{cases} . \tag{14}$$

When the PHEV finishes the mild braking period and the mechanical braking forces have not made the front or rear wheels being in critical locked state, the regenerative braking forces are decided by the ECE braking regulations and the constraint of anti-lock rear wheels. Eq.15 shows the strategy in this case.

$$\begin{cases} F_{b\_r\_re} \le \min\left\{F_{b\_r\_re\_\mathrm{ECE}}, F_{b\_r\_re\_\mathrm{ABS}}\right\} = F_{b\_r\_re\_\max} \\ F_{b\_r\_re} = \begin{cases} F_{re\_a}, & F_{re\_a} \le F_{b\_r\_re\_\max} \\ F_{b\_r\_re\_\max}, & F_{re\_a} > F_{b\_r\_re\_\max} \end{cases} \\ F_{b\_f\_sum} = F_{b\_f\_me} \\ F_{b\_r\_sum} = F_{b\_r\_me} + F_{b\_r\_re} \end{cases} . \tag{15}$$

When the PHEV finishes the mild braking period and the mechanical braking forces have made the front or rear wheels being in critical locked state, the regenerative braking forces are decided by the constraint of anti-lock rear wheels. Eq.16 shows the strategy in this case.

$$\begin{cases} F_{b\_r\_re} \le F_{b\_r\_re\_\mathrm{ABS}} = F_{b\_r\_re\_\max} \\ F_{b\_r\_re} = \begin{cases} F_{re\_a}, & F_{re\_a} \le F_{b\_r\_re\_\max} \\ F_{b\_r\_re\_\max}, & F_{re\_a} > F_{b\_r\_re\_\max} \end{cases} \\ F_{b\_f\_sum} = F_{b\_f\_me} \\ F_{b\_r\_sum} = F_{b\_r\_me} + F_{b\_r\_re} \end{cases} . \tag{16}$$

In a nutshell, the revised strategy can recover certain energy in some cases in the severe braking strategy.

4. Comparison of Recovery Rate

The recovery rate of the two strategies are compared when the PHEV with different strategies are running on the same road with the same drive intention and initial velocities.

When the traditional PHEV is in the mild and moderate braking periods, the revised PHEV has the same states with the traditional PHEV. So the recovered energy of the two strategies equal in these two periods.

$$Energy_{hev\_t} \_ partA = Energy_{hev\_r} \_ partA . \tag{17}$$

As is shown in the Eq.17, $Energy_{hev\_t} \_ partA$ is the recovered energy of the traditional PHEV in the mild and moderate braking periods; $Energy_{hev\_r} \_ partA$ is the recovered energy of the revised PHEV in the mild and moderate braking periods.

When the synchronizing adhesion coefficient is lower than the pavement friction coefficient, the pavement friction coefficient is lower than 0.7, and the traditional PHEV is in severe braking period, the revised PHEV has the same strategy with the traditional PHEV. So the recovered energy of the two strategies equal at this time.

$$Energy_{hev\_t} \_ partB = Energy_{hev\_r} \_ partB = 0 . \quad (18)$$

As is shown in the Eq.18, $Energy_{hev\_t} \_ partB$ is the recovered energy of the traditional PHEV in the severe braking periods; $Energy_{hev\_r} \_ partB$ is the recovered energy of the revised PHEV in the severe braking periods.

When the synchronizing adhesion coefficient is higher than the pavement friction coefficient and the traditional PHEV is in the severe braking period, the revised PHEV adds more regenerative braking forces than the traditional PHEV does. Eq.19 shows the recovered energy relations of the two PHEV at this time.

$$Energy_{hev\_r} \_ partB > Energy_{hev\_t} \_ partB = 0 . \quad (19)$$

When the pavement friction coefficient is higher than 0.7 and the traditional PHEV is in severe braking period, the revised PHEV adds more regenerative braking forces than the traditional PHEV does. Eq.20 shows the recovered energy relations of the two PHEV at this time.

$$Energy_{hev\_r} \_ partB > Energy_{hev\_t} \_ partB = 0 . \quad (20)$$

Eq.21 shows the recovered energy of the traditional PHEV during the whole braking process.

$$Energy_{hev\_t} = Energy_{hev\_t} \_ partA + Energy_{hev\_t} \_ partB . \quad (21)$$

As is shown in Eq.21, $Energy_{hev\_t}$ is the recovered energy of the traditional PHEV during the whole brake process.

Eq.22 shows the recovered energy of the revised PHEV during the whole braking process.

$$Energy_{hev\_r} = Energy_{hev\_r} \_ partA + Energy_{hev\_r} \_ partB . \quad (22)$$

As is shown in Eq.22, $Energy_{hev\_r}$ is the recovered energy of the revised PHEV during the whole brake process.

Eq.23 shows the relations of the recovered energy of the two strategies during the whole braking process.

$$Energy_{hev\_t} \le Energy_{hev\_r} . \quad (23)$$

Eq.24 shows the relations of the recovery rate of regenerative braking of the two strategies.

$$0 < \frac{Energy_{hev\_t}}{\frac{1}{2} M v_0^2} \le \frac{Energy_{hev\_r}}{\frac{1}{2} M v_0^2} < 1 . \quad (24)$$

As is shown in Eq.24, v_0 is the initial velocity.

It can be concluded from the Eq.24 that the revised strategy can recover more energy than the traditional one in some cases.

5. Comparison of Braking Distance

The braking distance of the two strategies are compared when the PHEV with the two strategies are running on the same road with the same drive intention and initial velocities.

When the traditional PHEV is in the mild and moderate braking periods, the revised PHEV has the same states with the traditional PHEV. So the braking distance of the two strategies equal in these two periods.

$$Distance_{hev\_t} \_ partA = Distance_{hev\_r} \_ partA . \quad (25)$$

As is shown in the Eq.25, $Distance_{hev\_t} \_ partA$ is the braking distance of the traditional PHEV in the mild and moderate braking periods; $Distance_{hev\_r} \_ partA$ is the braking distance of the revised PHEV in the mild and moderate braking periods.

When the synchronizing adhesion coefficient is lower than the pavement friction coefficient, the pavement friction coefficient is lower than 0.7, and the traditional PHEV is in the severe braking period, the revised PHEV has the same strategy with the traditional PHEV. So the braking distance of the two strategies equal at this time.

$$Distance_{hev\_t} \_ partB = Distance_{hev\_r} \_ partB. \quad (26)$$

As is shown in the Eq.26, $Distance_{hev\_t} \_ partB$ is the braking distance of the traditional PHEV in the severe braking periods; $Distance_{hev\_r} \_ partB$ is the braking distance of the revised PHEV in the severe braking periods.

When the synchronizing adhesion coefficient is higher than the pavement friction coefficient and the traditional PHEV is in severe braking period, the revised PHEV adds more regenerative braking forces than the traditional PHEV does. The revised PHEV has higher braking severity than the traditional PHEV does. Eq.27 shows the braking distance relations of the two PHEV at this time.

$$Distance_{hev\_t} \_ partB > Distance_{hev\_r} \_ partB. \quad (27)$$

When the pavement friction coefficient is higher than 0.7 and the traditional PHEV is in the severe braking period, the revised PHEV adds more regenerative braking forces than the traditional PHEV does. The revised PHEV has higher braking severity than the traditional PHEV does. Eq.28 shows the braking distance relations of the two PHEV at this time.

$$Distance_{hev\_t} \_ partB > Distance_{hev\_r} \_ partB. \quad (28)$$

Eq.29 shows the braking distance of the traditional PHEV during the whole braking process.

$$Distance_{hev\_t} = Distance_{hev\_t} \_ partA + Distance_{hev\_t} \_ partB. \quad (29)$$

As is shown in Eq.29, $Distance_{hev\_t}$ is the braking distance of the traditional PHEV during the whole brake process.

Eq.30 shows the braking distance of the revised PHEV during the whole braking process.

$$Distance_{hev\_r} = Distance_{hev\_r} \_ partA + Distance_{hev\_r} \_ partB. \quad (30)$$

As is shown in Eq.30, $Distance_{hev\_r}$ is the braking distance of the revised PHEV during the whole brake process.

Eq.31 shows the relations of the braking distance of the two strategies.

$$Distance_{hev\_t} \geq Distance_{hev\_r}. \quad (31)$$

It can be concluded from the Eq.31 that the revised strategy can shorten the braking distance in some cases.

6. Establishment of Braking Strategy Model

On the basis of MATLAB/ SIMULINK platform, the braking models of the traditional and the improved strategies are established.

Figure 1 shows the operating flowchart of the traditional method. Figure 2 shows the operating flowchart of the improved strategy.

In Fig.1, when the driver's expected braking intensity is less than 0.1, the mechanical braking force do not play a role in the braking process. Meanwhile, the mechanical braking forces of the front and rear wheels are zero. Under this condition, the value of the braking force is solely based on the regenerative braking force which is applied on the rear wheels. The specific values can be calculated by the instantaneous vehicle speed and the motor modules. The transient braking intensity in this case is calculated by the regenerative braking force, because the mechanical braking force is zero. The instantaneous speed is calculated by the instantaneous intensity and the vehicle initial speed.

When the expected braking force is higher than 0.7, it can be considered as a case of severe braking process and the regenerative braking is not operating in this process. From the comparison between the synchronous and road adhesion coefficient, the approach to calculate the braking efficiency is selected. Hence, the braking efficiency of the certain road adhesion coefficient can be obtained.

Therefore, the maximum mechanical braking force can be calculated in the case that the front and rear wheels are not locking. In the severe braking process, the value of instantaneous braking severity of the vehicle is between 0.7 and the maximum mechanical braking severity under the premise that the front and rear wheels are not locking.

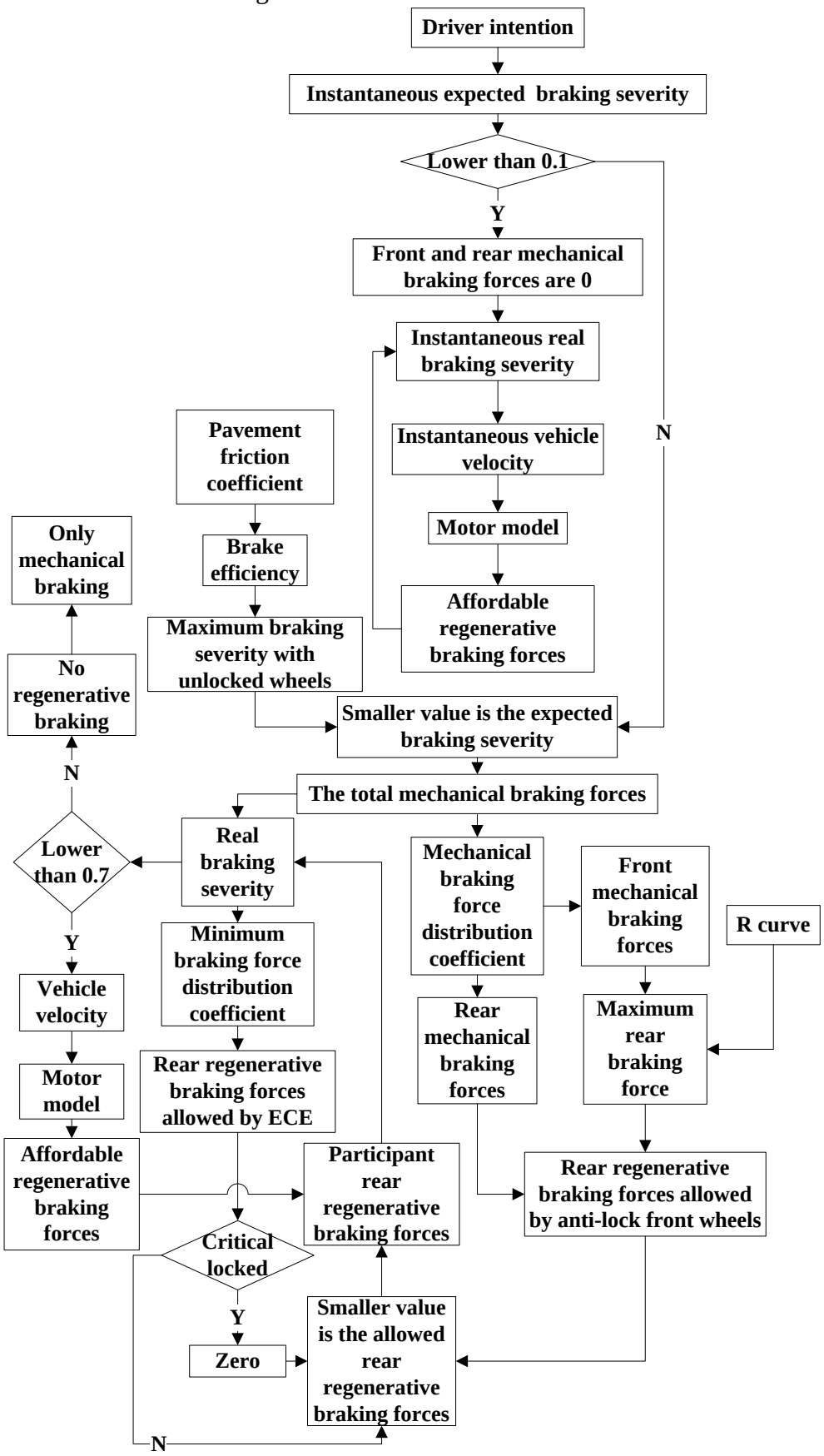

Fig. 1 Flowchart of traditional strategy

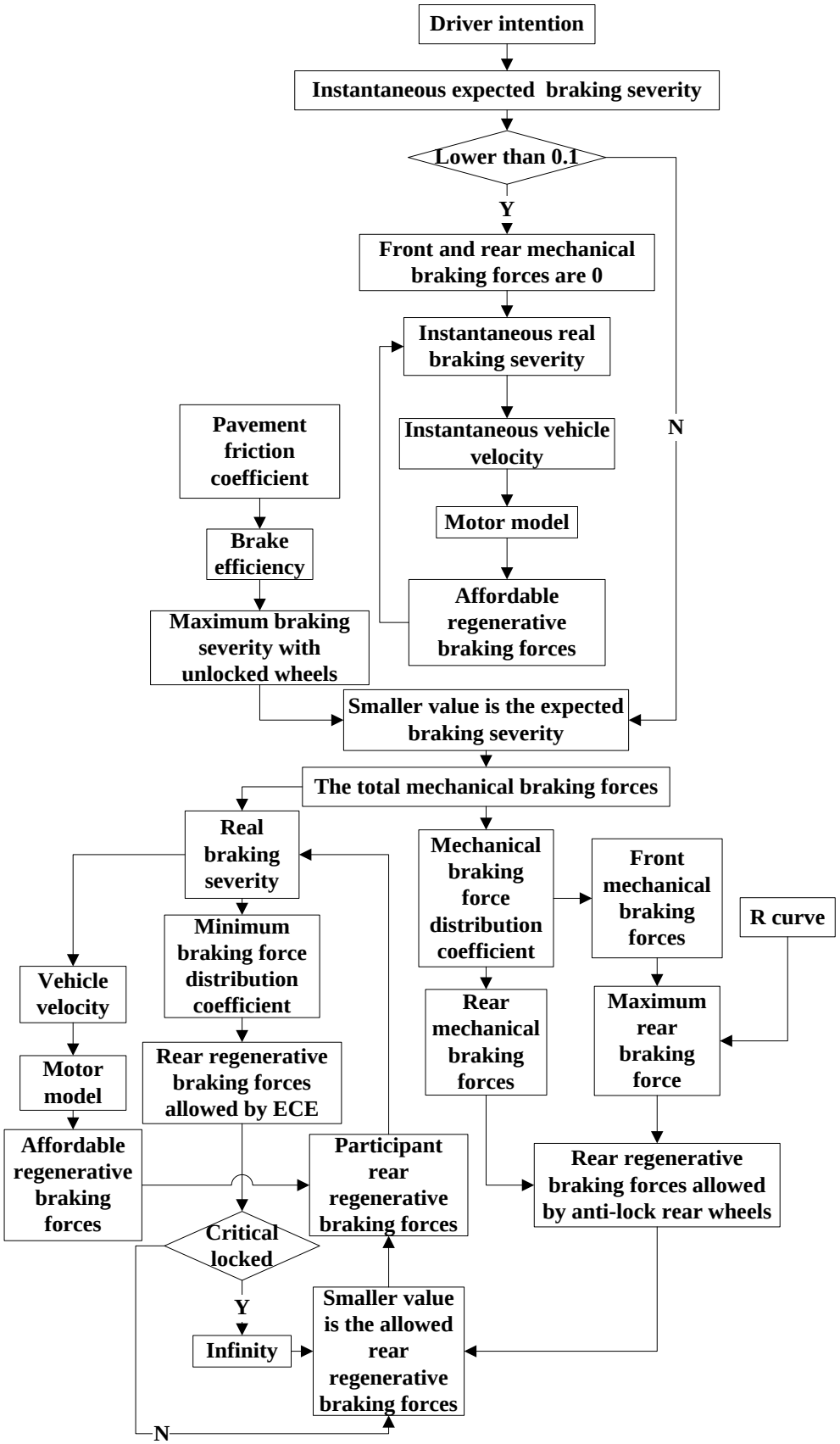

Fig. 2 Flowchart of improved strategy

When the expected value of the braking severity is between 0.1 and 0.7, it includes the moderate braking process and the other case of the severe braking process. The regenerative braking forces are determined by the constraints of ECE regulations and preventions of rear wheels locking. In the situation that the front or rear wheels are in critical locking states, constraints of ECE regulations and preventions of rear wheels locking loss efficacy simultaneously and the regenerative braking force

disappears as well. This specific idea reflected in the braking model is the operation that the allowed rear regenerative braking forces are 0 when the front or the rear wheels are critically locked by the mechanical braking forces. The regenerative braking force is the minimum value between the values of rear wheels locking constraints and ECE constraints. Therefore, when this value is assigned to 0, the system stops the participation of the regenerative braking force, which simulates the mentioned the other case of the severe braking process. In the moderate braking process, the braking force would not make the front or rear wheels being critically locked states. So the regenerative braking force allowed by rear wheels locking constraints would not be assigned to 0. Thus, it can also simulate the situation of the moderate braking process. When the braking severity expectation is between 0.1 and 0.7, the instantaneous braking severity can be calculated by the mechanical braking force of front and rear wheels and the regenerate braking force. The instantaneous velocity can be calculated by the instantaneous braking severity and the value is useful for circularly importing into other modules.

The actual braking distance can be jointly calculated by three parts of actual braking severity. The recovered energy during the braking process can be calculated through integrating the product of regenerative braking force and instantaneous vehicle speed. The total energy of the braking process can be obtained by the integration of the product of braking severity, vehicle weight and the instantaneous vehicle speed.

In figure 2, the models of the moderate and one case of the severe braking process have the same executions with the traditional strategy. The constraints of ECE regulations not always operate throughout the braking process. When the front or rear wheels are in the critical locked state, the constraints of ECE regulations are terminated, which is achieved by assigning the infinite value to the regenerative braking force allowed by ECE regulations. At this time, it is eliminated by comparing with the Rear-wheel anti-locking constraints. Anti-rear locking constraints, which need to use curve R to calculate, always exist in the whole braking process.

7. Analyses of Simulation Results

In order to compare the braking distance of the two strategies, the driver intention adopts the process of slowly stepping on the brake pedal instead of the frequently-used driving cycles. The process of slowly stepping on the brake pedal contains the mild braking period, the moderate braking period and the severe braking period. Eq.32 shows the adoptive driver intention in the models.

$$F_{driver} = \int H dt . \tag{32}$$

As is shown in Eq.32, F_{driver} is the driver's expectation of braking force; H is growth rate of the braking force.

Table 2 Parameters

Parameters	Value
Wheel base of PHEV [m]	5.6
Distance between front axle and the mass center [m]	3.733
Distance between rear axle and the mass center [m]	1.867
Height of center of mass [m]	1
Mass of PHEV [kg]	5800
Wheel radius [m]	0.52
Power of DC motor [kW]	60
Synchronizing adhesion coefficient	0.65
Mechanical braking force distribution coefficient	0.4495
Initial velocity [km/h]	50

When the pavement friction coefficient is 0.5, which is lower than the threshold 0.7 and lower than the synchronizing adhesion coefficient, the two models, embed the parameters shown in Table 2, were simulated. The simulation results are shown from Fig.3 to Fig.7. In detail: Fig.3 shows the rear

regenerative braking forces; Fig.4 shows the braking severity; Fig.5 shows the braking force distribution coefficient; Fig.6 shows the recovered energy; Fig.7 shows the braking distance.

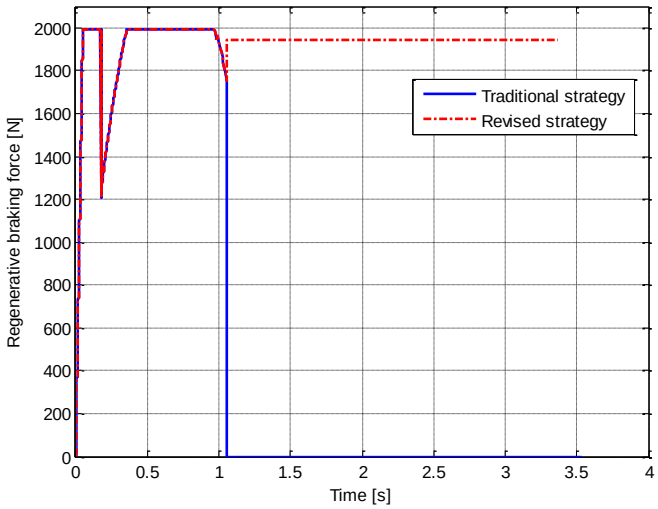

Fig.3 Instantaneous regenerative braking force on rear wheels

Fig.3 shows that the rear regenerative braking force of the two strategies had the same operations during the mild and moderate braking processes. During the severe braking process, the traditional strategy no longer provided the regenerative braking force. However, the revised strategy provided the regenerative braking force during the whole braking process.

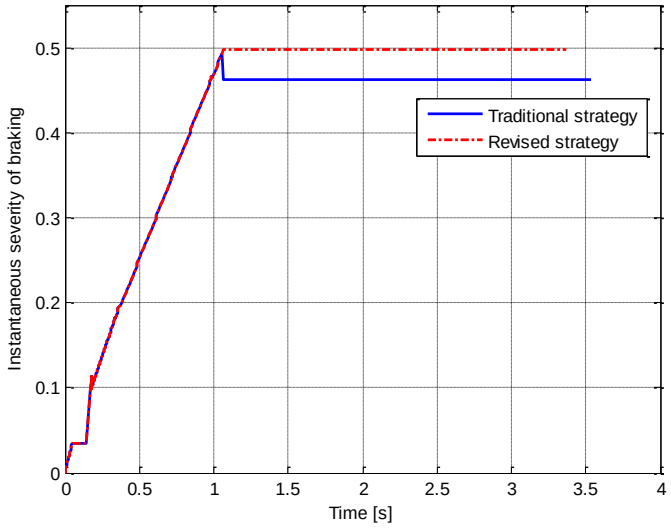

Fig.4 Instantaneous severity of braking

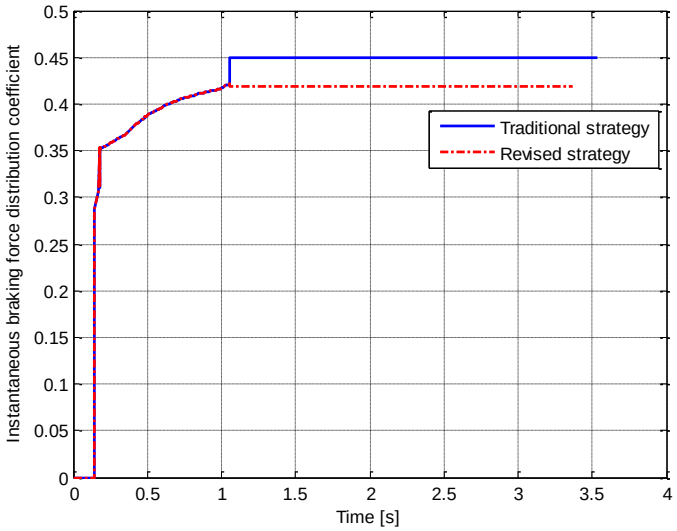

Fig.5 Instantaneous braking force distribution coefficient

Fig.4 shows that the instantaneous severity of braking of the two strategies had the same states during the mild and moderate braking processes. During the severe braking process, the braking severity of the revised strategy was higher than that in the traditional strategy. This is because there were regenerative braking forces adding onto the rear wheels in the severe braking period. Then the rear regenerative braking forces made the rear wheels being in the critical locked state in the severe period and thus the braking severity equalled the pavement friction coefficient.

Fig.5 shows that the instantaneous braking force distribution coefficient of the two strategies had the same values during the mild and moderate braking processes. During the severe braking process, the instantaneous braking force distribution coefficient of the revised strategy was lower than that in the traditional strategy. In addition, the instantaneous braking force distribution coefficient of the traditional strategy during the severe braking period equalled the mechanical braking force distribution coefficient, while the counterpart of the revised strategy was lower than the mechanical braking force distribution coefficient. This is because the revised strategy provided the regenerative braking forces during the severe braking period.

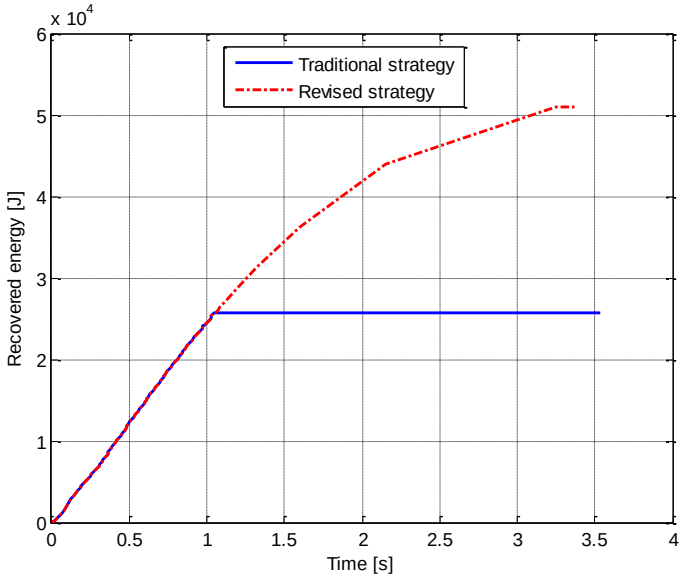

Fig.6 Recovered energy

Fig.6 shows that the traditional strategy did not recover the energy in the severe braking period. However, the revised strategy was recovering the energy during the whole braking process.

Fig.7 shows that the braking distance of the traditional strategy was the same with the counterpoint of the revised strategy in the mild and moderate braking periods. In addition, the traditional strategy had longer braking distance than the revised strategy in the severe braking period.

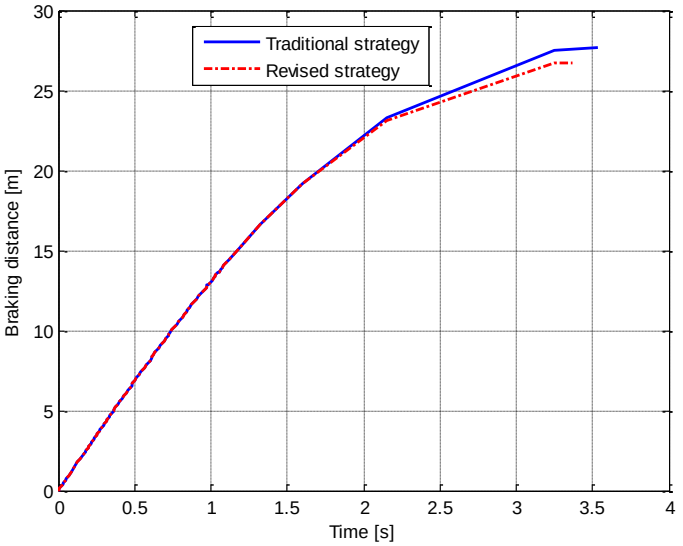

Fig.7 Braking distance

When the pavement friction coefficient is 0.8, which is higher than the threshold 0.7 and higher than the synchronizing adhesion coefficient, the two models, embed the parameters shown in Table 2, were simulated. The simulation results are shown from Fig.8 to Fig.12. In detail: Fig.8 shows the rear regenerative braking forces; Fig.9 shows the braking severity; Fig.10 shows the braking force distribution coefficient; Fig.11 shows the recovered energy; Fig.12 shows the braking distance.

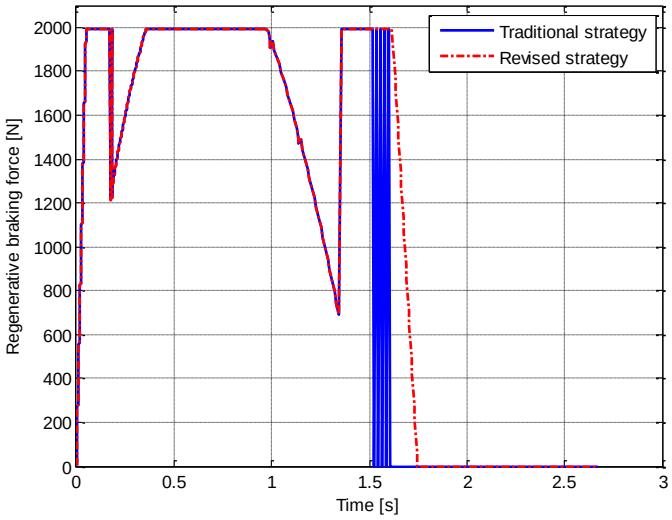

Fig.8 Instantaneous regenerative braking force on rear wheels

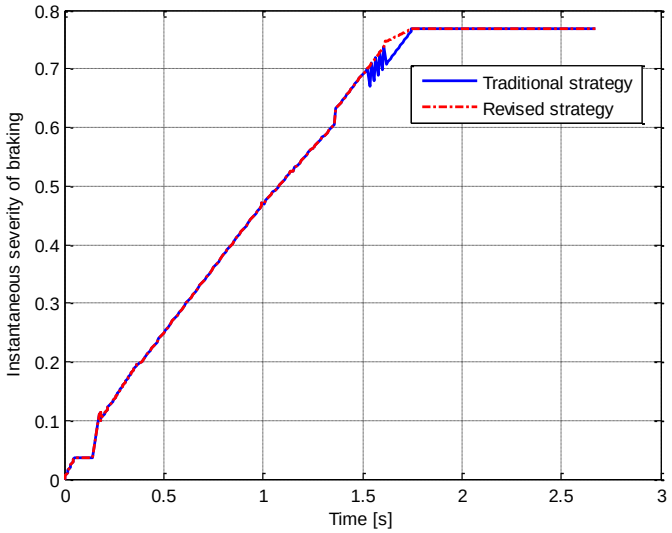

Fig.9 Instantaneous severity of braking

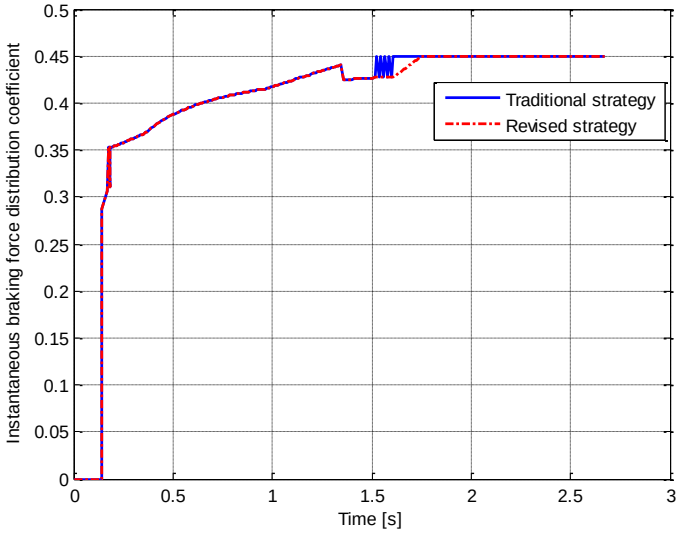

Fig.10 Instantaneous braking force distribution coefficient

Fig.8 shows that the rear regenerative braking force of the two strategies had the same operations during the mild and moderate braking processes. During the severe braking process, the traditional strategy no longer provided the regenerative braking force. However, the revised strategy provided the regenerative braking force in the earlier stage of the severe braking period. This operation continued until the rear wheels stepped into the critical locked state.

Fig.9 shows that the instantaneous severity of braking of the two strategies had the same states during the mild and moderate braking processes. The braking severity of the revised strategy was higher than that in the traditional strategy in the earlier stage of the severe braking period.

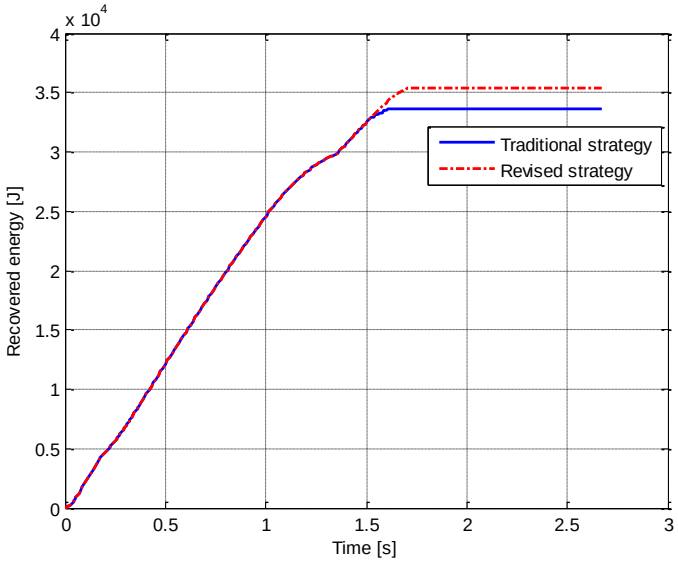

Fig.11 Recovered energy

Fig.10 shows that the instantaneous braking force distribution coefficient of the two strategies had the same values during the mild and moderate braking processes. The instantaneous braking force distribution coefficient of the revised strategy is lower than that in the traditional strategy in the earlier stage of the severe braking period. Finally, the instantaneous braking force distribution coefficient of the two strategies equal the mechanical braking force distribution coefficient.

Fig.11 shows that traditional strategy did not recover energy in severe braking period. However, the revised strategy recovered energy in the earlier stage of the severe braking period and it would no longer recover energy after the rear wheels stepped into the critical locking state.

Fig.12 shows that the braking distance of traditional strategy was the same with the counterpoint of the revised strategy in the mild and moderate braking periods. In addition, the braking distance of the two strategies were different in the severe braking period.

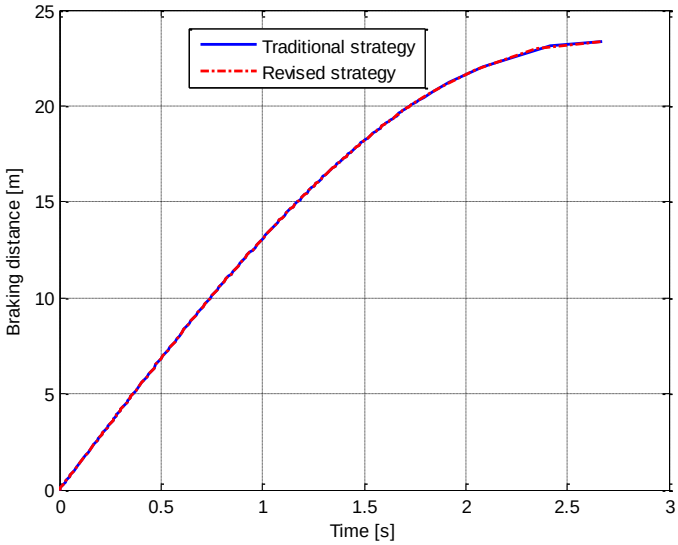

Fig.12 Braking distance

In order to evidently compare the differences of the braking distance between the two strategies during the severe braking period, part of the Fig.12 was enlarged. Fig.13 shows the partial enlarged detail.

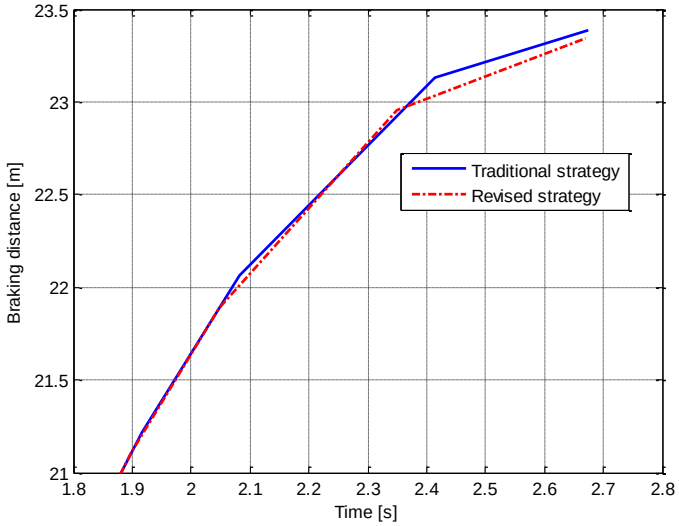

Fig.13 Partial enlarged detail of the braking distance

Fig.13 shows that the traditional strategy had longer braking distance than the revised strategy in the severe braking period.

Additionally, the two models, embed the parameters shown in Table 2, were simulated with different pavement friction coefficients. Table 3 shows the results.

The results in the Table 3 indicate that the revised strategy has considerable higher regenerative braking recovery rate and overt shorter distance when the pavement friction coefficient is lower than 0.65, which is lower than the synchronizing adhesion coefficient.

In addition, the revised strategy has slight higher regenerative braking recovery rate and minor shorter distance when the pavement friction coefficient is higher than 0.7, the threshold of the traditional strategy.

The revised strategy shares the same situations with the traditional one when the pavement adhesion coefficient is higher than 0.65 but lower than 0.7; There is no increase in the regenerative braking recovery rate or no decrease in the braking distance at this time.

Table 3 Simulation results with different pavement friction coefficients

Pavement friction coefficient	Traditional strategy recovery rate	Revised strategy recovery rate	Increment rate of recovery rate	Traditional strategy braking distance	Revised strategy braking distance	Decrement rate of braking distance
0.42	3.76%	10.34%	175.0%	31.49	29.76	5.49%
0.47	4.29%	9.60%	123.8%	28.90	27.69	4.19%
0.52	4.78%	8.56%	79.08%	27.01	26.25	2.81%
0.57	5.15%	7.21%	40.00%	25.64	25.27	1.44%
0.62	5.37%	6.04%	12.48%	24.66	24.55	0.45%
0.65	5.52%	5.52%	0.00%	24.18	24.18	0.00%
0.67	5.66%	5.66%	0.00%	24.04	24.04	0.00%
0.70	5.83%	5.83%	0.00%	23.82	23.82	0.00%
0.72	5.94%	5.95%	0.17%	23.70	23.69	0.04%
0.77	5.98%	6.19%	3.51%	23.47	23.45	0.09%
0.82	5.98%	6.43%	7.53%	23.32	23.26	0.26%
0.87	5.98%	6.63%	10.87%	23.20	23.12	0.34%

In order to evidently show the differences of the regenerative braking recovery rate of the two strategies with different values of pavement friction coefficient, the results in the Table 3 are

exhibited in the form of line graph. Fig.14 shows the trend of the regenerative braking recovery rate of the two strategies.

In order to evidently show the differences of the braking distance of the two strategies with different values of pavement friction coefficient, the results in the Table 3 are exhibited in the form of line graph. Fig.15 shows the trend of the braking distance of the two strategies.

In order to evidently compare the differences of the braking distance between the two strategies when the the pavement friction coefficient is higher than 0.7, part of the Fig.15 was enlarged. Fig.16 shows the partial enlarged detail.

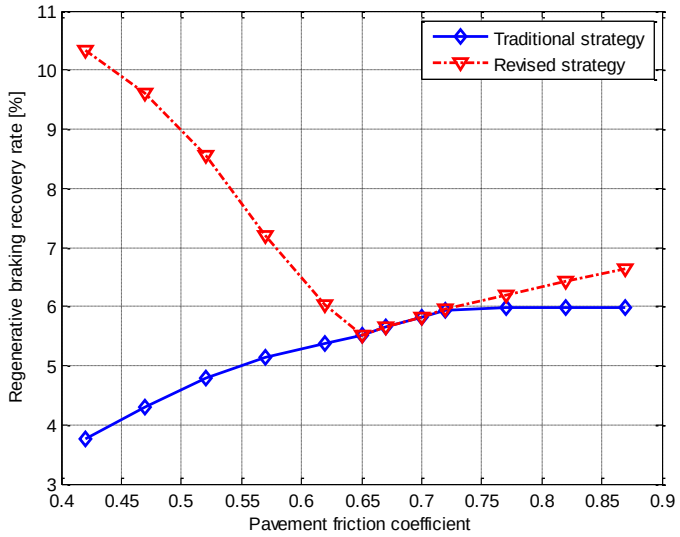

Fig.14 Regenerative braking recovery rate of the two strategies

Fig.14 indicates that the revised strategy has higher regenerative braking recovery rate when the the pavement friction coefficient is lower than 0.65 or higher than 0.7. When the the the pavement friction coefficient is between 0.65 and 0.7, the regenerative braking recovery rate of the two strategies share the same values.

Fig.15 indicates that the revised strategy has shorter braking distance when the the pavement friction coefficient is lower than 0.65. When the the the pavement friction coefficient is between 0.65 and 0.7, the braking distance of the two strategies share the same values.

Fig.16 indicates that the revised strategy has shorter braking distance when the the pavement friction coefficient is higher than 0.7.

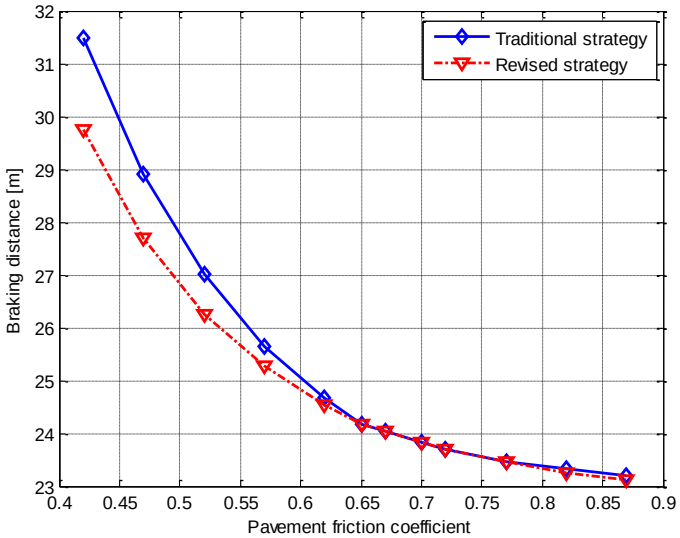

Fig.15 Braking distance of the two strategies

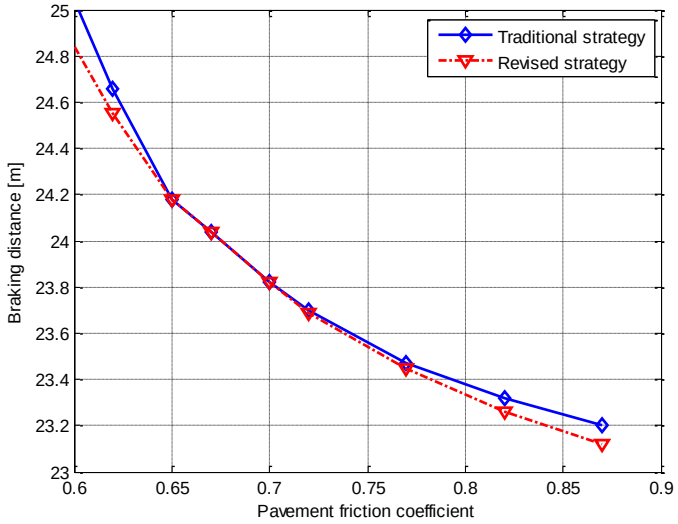

Fig.16 Partial enlarged detail of the braking distance of the two strategies

8. Conclusion

The study object is the parallel hybrid electric commercial cars with rear-wheel drive pattern. The traditional strategy was revised and the novel strategy can recover braking energy in the severe braking period in some cases. In these cases, the PHEV with the revised strategy can not only increase the regenerative braking recovery rate but also shorten the braking distance.

Compared with the traditional strategy, when the pavement friction coefficient is higher than the threshold value 0.7, the regenerative braking recovery rate of the revised strategy has a slight increase and the braking distance of the revised strategy has a minor decrease.

Compared with the traditional strategy, when the pavement friction coefficient is lower than the synchronizing adhesion coefficient, the regenerative braking recovery rate of the revised strategy has an obvious increase and the braking distance of the revised strategy has a great decrease. The revised strategy in this case is quite suitable for the wet ground in the summer season.

References

[1] J.M. Zhang, J.L. Liu, and M.Z. Xue: Analyses of the Relation between Degree of Mixing and Regenerative Braking in Hybrid Electric Vehicles, Advanced Materials Research, Vol. 926, 2014.

[2] J.L. Liu, Jing J.M. Zhang and Ming M.Z. Xue: Analyses of Relations between Pavement Adhesion Coefficient and Regenerative Braking in Hybrid Electric Vehicle, Applied Mechanics and Materials 536 (2014): 1065-1068.

[3] J.L. Liu, Z.W. Gao, J.M. Zhang: Analyses of the Relations Between Driving Types and Regenerative Braking in Electric Vehicles, Advanced Materials Research, Vol. 926, 2014.

[4] J.L. Liu, J.M. Zhang and M.Z. Xue: A Novel Parallel Regenerative Braking Control Strategy, Journal of applied science and engineering innovation, Vol.1.4 (2014).

[5] J.L. Liu,, X.Y. Zhang, and R. Huang: Impacts of PHEV Driving Types on Electro-hydraulic Braking, Journal of Computational Science & Engineering, Vol. 12. 2014.

[6] J.L. Liu, J.M. Zhang, and Z.W. Gao: The Energy Management and Coordination in PHEV, Journal of applied science and engineering innovation Vol.1.4 (2014).